PAPER

Check for updates

Conductive MXene ultrafiltration membrane for improved antifouling ability and water quality under electrochemical assistance†

Lulu Qian, Chengyu Yuan, Xu Wang, Haiguang Zhang, Lei Du, Gaoliang Wei and Shuo Chen [iD] *

Membrane fouling is a major challenge for the membrane separation technique in water treatment. Herein, an MXene ultrafiltration membrane with good electroconductivity and hydrophilicity was prepared and showed excellent fouling resistance under electrochemical assistance. The fluxes under negative potential were 3.4, 2.6 and 2.4 times higher than those without external voltage during treatment of raw water containing bacteria, natural organic matter (NOM), and coexisting bacteria and NOM, respectively. During the treatment of actual surface water with 2.0 V external voltage, the membrane flux was 1.6 times higher than that without external voltage and the TOC removal was improved from 60.7% to 71.2%. The improvement is mainly attributed to the enhanced electrostatic repulsion. The MXene membrane presents good regeneration ability after backwashing under electrochemical assistance with the TOC removal remaining stable at around 70.7%. This work demonstrates that the MXene ultrafiltration membrane under electrochemical assistance possesses excellent antifouling ability and has great potential in advanced water treatment.

1. Introduction

Membrane separation, as one of the water purification technologies, is widely used in advanced wastewater treatment because of its simple operation, stable performance and compact structure.[1–5] However, membrane fouling is an unavoidable problem because of the complex composition of feed water containing pathogens and organic matter, which generally leads to a deterioration in membrane performance, especially decreased permeability.[6–8]

At present, the prevention and control measures of membrane fouling mainly include the setting of pretreatment facilities and the investigation of anti-fouling membrane.[9,10] Sewage pretreatment can alleviate the loss of subsequent treatment equipment, but it will inevitably increase the operating cost. Various strategies, such as membrane modification, optimization of operating conditions and coupling with other technologies to construct functional membranes, are devoted to improving the antifouling performance of the membranes.[11–14] In reported works, the introduction of electrochemical technology into membrane separation may be an effective strategy

Key Laboratory of Industrial Ecology and Environmental Engineering (Ministry of Education, China), School of Environmental Science and Technology, Dalian University of Technology, Dalian, 116024, China. E-mail: shuochen@dlut.edu.cn; Tel: +86-411-84706263

† Electronic supplementary information (ESI) available. See DOI: https://doi.org/10.1039/d3ra01116j

to mitigating the membrane fouling.[15–17] Thus, membrane made of conductive materials have received a lot of attention.[18–20]

MXene materials, which have been widely studied since it was first reported in 2011, shows great potential applications in diverse fields such as energy storage devices, adsorption and photocatalysts.[21–28] Meanwhile, MXene as a novel type of membrane materials has also been constructed into selective separation membrane, which has been examined to be efficient in water treatment.[29–31] MXene has hydrophilicity and inherent conductivity, which provides the possibility for the construction of electroconductive membranes, and their performance in antifouling and rejection is expected to be improved under electrochemical assistance.[32,33] It can be speculated that enhanced electrostatic repulsion would make contaminants with same charge keep away from the membrane surface, thus mitigating membrane fouling. If the fascinating electrochemical properties can be introduced into MXene membranes, the additional electrochemical functions would slow down or prevent the transmembrane transport of contaminants. This might be an effective approach to improve the antifouling ability for MXene membranes.

Currently, MXene membranes have received significant attention in nanofiltration (NF) owing to its unique physicochemical properties.[34,35] The risk of membrane fouling in ultrafiltration (UF) membranes is greater than NF membranes, because there is usually pretreatment, for instance microfiltration or ultrafiltration, for NF membranes to mitigate

fouling.[36] UF membranes are mainly aimed at removing pathogens, NOM and other substances from sewage according to the principle of pore size sieving, which is easy to form membrane fouling in the filtration process as a result of bacterial multiplication and NOM accumulation.[37] Moreover, it has been reported that polyaniline (PANI) and TiCT (MXene) were combined to prepare conductive mixed ultrafiltration membrane, and bovine serum albumin (BSA) was used to investigate the anti-fouling ability of composite membrane under electric field.[38] On this basis, it is necessary to further investigate the antifouling ability of the membrane for different fouling types under electrochemical assistance.

Herein, to verify the feasibility of the above strategy, an electroconductive MXene membrane in ultrafiltration scale was prepared by coating multi-layered MXene onto ceramic substrate *via* a vacuum filtration method. Effects of negative bias on the resistance to biofouling and organic fouling for membrane were examined. Filtration experiments were also performed under negative electrochemical assistance coexisting bacteria and natural organic matter (NOM). In addition, performance for the treatment of surface water was also investigated, which provided a reliable research basis for the practical application of electrochemically assisted membrane separation process.

2. Experimental

2.1 Fabrication of MXene ultrafiltration membrane

In a typical membrane fabrication method, a vacuum filtration process was used to construct MXene functional layers on a porous Al_2O_3 substrate (Fig. S1†). Firstly, multi-layered $Ti_3C_2T_X$ was obtained *via* etching Al element of Ti_3AlC_2 with a LiF–HCl solution.[39] 1.0 g LiF was added to 20 mL HCl (9 M) in a PTFE vessel. 1.0 g of Ti_3AlC_2 powders (Beike Nano Co., Ltd, Suzhou, China) was dissolved in the above solution under stirring (300 rpm). Etching was performed for 48 h at 60 °C. Then, the mixture was washed many times with ultra-pure water by centrifugation at 3500 rpm. Subsequently, the suspension was collected by centrifugation at 3500 rpm for 20 min to remove large unetched Ti_3AlC_2. Finally, the concentrated MXene solution was conserved under Ar atmosphere at 4 °C. To provide mechanical strength for membrane, the multi-layered MXene was vacuum-filtered onto a ceramic substrate and dried at room temperature.

2.2 Characterization of multi-layered MXene and MXene membrane

The observation of membrane morphologies was obtained by a field-emission scanning electron microscope (SEM, SU5000, Hitachi, Japan) equipped with an energy dispersive X-ray spectroscopy (EDS). X-ray photoelectron spectroscopy (XPS, ESCALAB250Xi, Thermo Fisher, UK) was used to characterize the materials chemistry. X-ray diffractometer (XRD, D8 Advance, Bruker Optics, Germany) was utilized to investigate the crystal structures of samples. The chemical structure was characterized by Fourier transform infrared spectrum (FTIR, VERTEX 70,

Bruker Optics, Germany). Membrane pore size distributions were determined by the Capillary Flow Porometer (POROLUX™ 1000, IB-FT GmbH, USA). Optical contact angle meter (CAST V2.28, Solon, USA) was used to measure water contact angle. TOC analyzer (multi N/C 2100S, Jena, Germany) was used to analyze TOC content in sample. The conductivity of the membrane was measured by a multifunction digital four-probe tester (ST-2258C, Suzhou, China).

2.3 Filtration experiments

The membrane performance was tested using a lab-made filtration setup (Fig. S2†). The membrane diameter was 38 mm and cross-flow rate was maintained at 0.18 m s^{-1} during the filtration processes (Fig. S3a†). The transmembrane pressure was controlled at 0.4 bar. Membrane performance was investigated under negative bias in an electrochemical system (cathode: MXene membrane, anode: titanium mesh) (Fig. S3b†). The permeate flux was monitored and the fouling of membrane surface was observed to evaluated membrane antifouling performance during filtration processes.

The common *Escherichia coli* (*E. coli*) were selected for anti-biofouling experiment. The *E. coli* strains were cultured into 200 mL of sterile Luria-Bertani (LB) liquid medium overnight on a constant temperature shaker at 35 °C with 121 rpm. Then, the obtained organisms were washed with sterilized physiological saline solution. Finally, the *E. coli* were redistributed in normal saline with a concentration of 10^7 colony forming units per milliliter (CFU mL^{-1}). The permeate water was collected and analyzed for colony number by coating plate counting method.

Humic acid (HA), as a kind of common NOM, was selected for anti-organic fouling experiment. The HA (Aladdin Reagents Co., Ltd, Shanghai) content in influent was 10 mg L^{-1}. Effluent sample was collected and analyzed for HA content using ultraviolet spectrophotometry (SP-756P, Spectral Instrument Co., Ltd, Shanghai) at 254 nm. In antifouling experiments, raw water contained 10^4 CFU mL^{-1} *E. coli* and 10 mg L^{-1} HA. Data were presented as the average values of three repetitive experiments. The permeate flux and rejection were obtained by following equations:

$$J = \frac{\Delta V}{T \times A \times P} \tag{1}$$

$$R = \frac{C_f - C_p}{C_f} \times 100\% \tag{2}$$

where J is membrane permeate flux (L m^{-2} h^{-1} bar^{-1}), ΔV is volume of permeation (L) under the applied pressure P (bar) within time T (h), A is the actual infiltration area (m^2), R is the rejection rate, C_f and C_p are the concentrations of feed and permeate (mg L^{-1}), respectively.

3. Result and discussion

3.1 Membrane characterization

As shown in Fig. 1a and b, Ti_3AlC_2 with a tight lump state is transformed into loose multi-layered $Ti_3C_2T_X$ by etching away middle Al layer. After chemical etching, the binding force
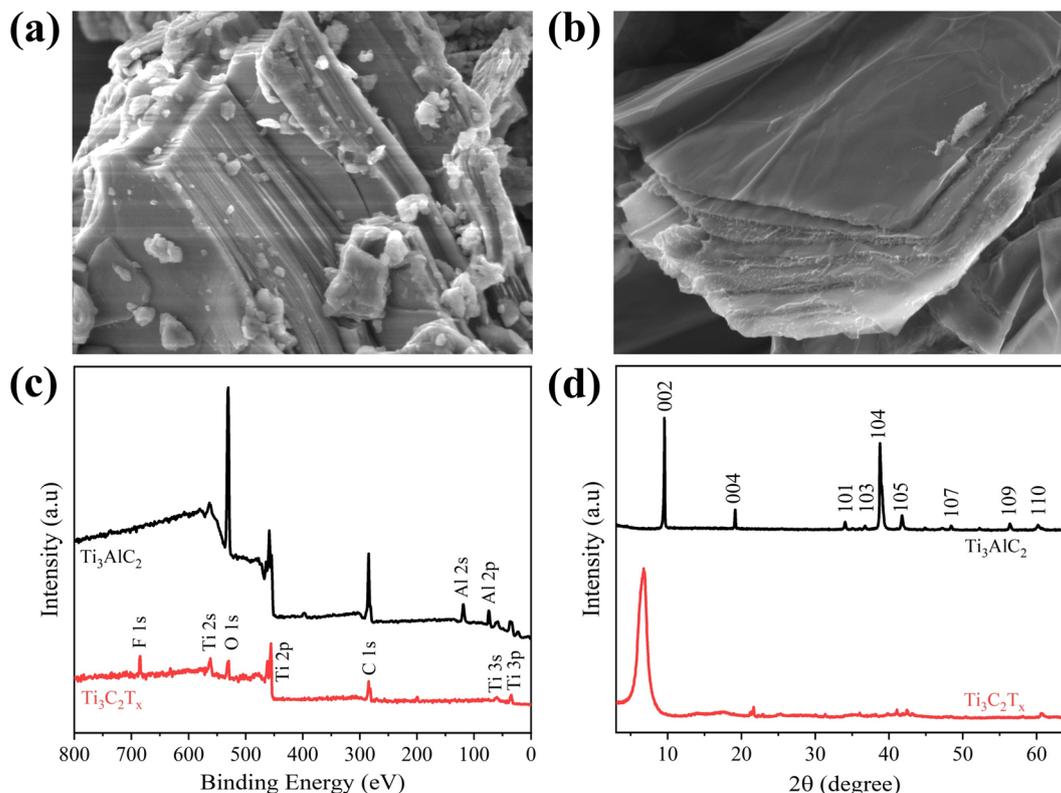
Fig. 1 SEM images of (a) Ti_3AlC_2 and (b) multi-layered $Ti_3C_2T_X$, (c) XPS spectra and (d) XRD patterns of Ti_3AlC_2 and $Ti_3C_2T_X$.

between $Ti_3C_2T_X$ lamellas is weakened, and further centrifugation leads to the slip between the layers, forming a separate multi-layered structure. And the surface of multi-layered $Ti_3C_2T_X$ is flat with no obvious wrinkles, indicating that it has good rigidity. XPS (Fig. 1c) verifies the removal of Al layers and the disappearance of 104 diffraction peak in XRD results also confirms the successful etching of Al element (Fig. 1d).[39,40] The presence of –O and –OH terminations on the surface of MXene is confirmed (Fig. S4 and S5†).[41,42] Multi-layered $Ti_3C_2T_X$ are evenly dispersed in water (Fig. S6†) with hydrophilic and negative surface charge, which is attributed to oxygen-containing functional groups.[43,44] Moreover, EDS mappings show that Ti, C, O and F elements are distributed on material surface (Fig. S7†).

3.2 Membrane performance control

Before the preparation of MXene membrane, the permeability of the unmodified ceramic substrate was investigated. And its pure water flux was 3035.2 L m^{-2} h^{-1} bar^{-1}, suggesting that it has good permeability and can be used as a substrate for MXene material. The membrane was prepared with different MXene loading. The loading of membrane material directly influences its selectivity and permeation. To optimize the loading of separation layer, the MXene amount was controlled and the results were shown in Fig. 2a. The membrane water flux decreased from 801.3 L m^{-2} h^{-1} bar^{-1} to 180.7 L m^{-2} h^{-1} bar^{-1} and rejection rate of HA improved from 31.7% to 91.1% with MXene loading increase. The HA rejection rate of unmodified

ceramic substrate was only 15.6% (Fig. S8†), while HA rejection rate of MXene membrane was as high as 86.5%. Considering membrane separation selectivity and water permeability, MXene loading with 2.33 mg cm^{-2} was selected as the optimal conditions to prepare MXene membrane, because it can not only provide good permeability, but also good rejection (86.5%) toward HA.

Compared with commercial membranes (PVDF membrane and CA-CN membrane), the prepared MXene membrane has remarkable hydrophilicity and good antifouling performance (Fig. S9 and S10†). There is a good linear relationship between pure water flux and operating pressure, indicating that the membrane has good pressure resistance (Fig. S11†). And the pure water flux of MXene membrane is 331.9 L m^{-2} h^{-1} at 1.0 bar.

As presented in EDS mapping, a MXene layers can be found in cross section of the membrane (Fig. S12†). It can be observed that ceramic substrate is a microfiltration membrane (average pore size: 241 nm), and the average pore size of as-fabricated membrane is 78 nm at ultrafiltration scale (Fig. 2b). As exhibited in Fig. 2c, membrane surface has no obvious defects with hydrophilicity (average water contact angle: 23°, inset of Fig. 2c). Moreover, the membrane possesses a good electrical conductivity of 2×10^5 S m^{-1}. Assembling the membrane into simple electric circuit can light up LED lights (inset of Fig. 2d), indicating that it can act as an electrode for applying electrical assistance in subsequent antifouling experiments.
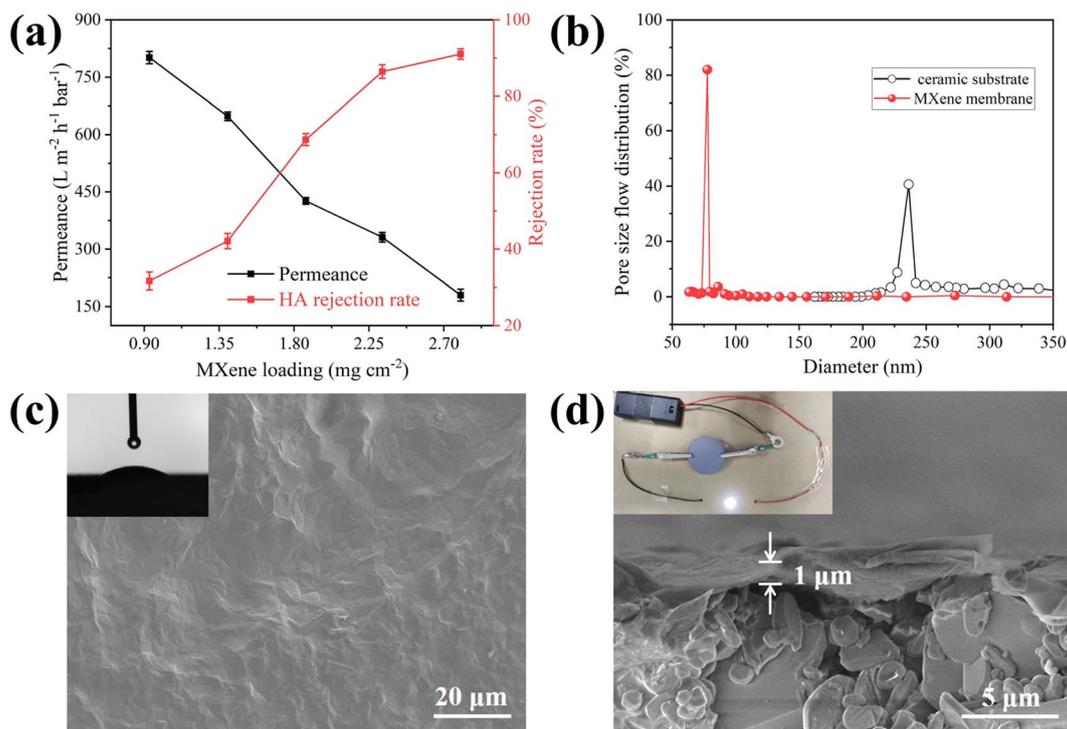
Fig. 2 (a) Pure water flux and HA rejection rates of MXene membranes with different MXene loadings, (b) pore size distribution of pristine ceramic substrate and the MXene membrane, SEM images of (c) surface and water contact angle (the inset), (d) cross section and good conductivity (the inset) of MXene membrane.

3.3 Electro-assisted membrane fouling mitigation

Before the experiment, membrane open circuit potential and Linear Voltammetry (LV) curve were tested to select the appropriate applied voltage. When 2.5 V was applied, MXene membrane cathode potential was −1.3 V (*vs.* Ag/AgCl, Fig. 3a). From the LV curve (Fig. 3b), hydrogen evolution reaction took place at −1.1 V (*vs.* Ag/AgCl). In order to avoid electrochemical reaction, the maximum applied voltage was 2.0 V in experiment. Meanwhile, the electrochemical stability of MXene membrane cathode was also investigated. 20 cycles of CV scans were measured at range of −1.2 V to +0.2 V (*vs.* Ag/AgCl). As shown in

Fig. S13,† all CV curves overlapped well. These results demonstrated that electrochemical properties of MXene membrane were stable, providing a guarantee for the subsequent electrically assisted experiments. Moreover, the influence of applied potentials on permeability of MXene membrane was investigated. As shown in Fig. S14,† there was no significant change for MXene membrane in pure water flux under different voltages, indicating that the applied potentials had no obvious interaction with the transmission of water molecules, thus the effect of electrochemical assistance on pure water permeability for MXene membrane could be ignored.
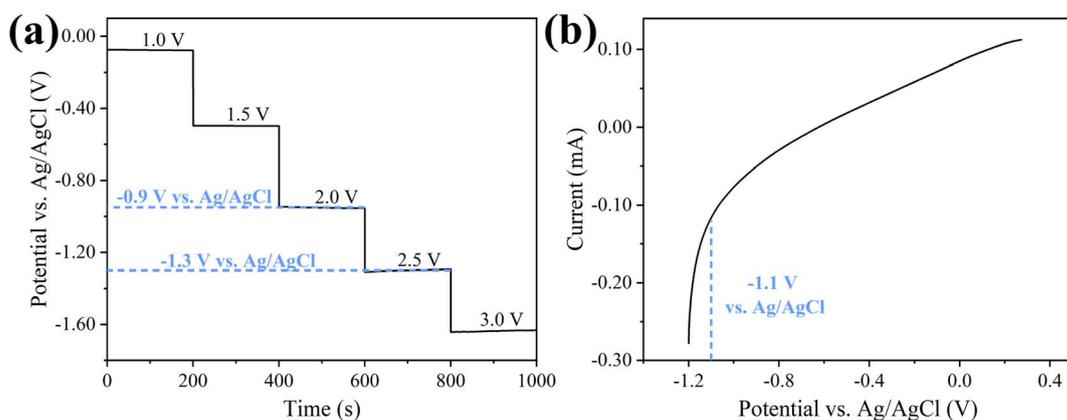

Fig. 3 (a) Cathode potential of MXene ultrafiltration membrane at different external voltage and (b) linear voltammetry curve of MXene ultrafiltration membrane as cathode.

The effect of negative bias on membrane for anti-biofouling ability was investigated by filtering raw water containing *E. coli*. The filtrate was collected and 50 μL permeate sample was coated over an agar plate and cultured at constant temperature oscillator for 24 h. The normalized flux during 120 min operating time was presented in Fig. 4a. The membrane permeability decreased sharply with time because of the formation of biofouling on membrane. A flux loss of 75.8% occurred after 120 min of operation without electro-assistance. However, the flux loss was decreased to 46.3% under 1.0 V electrochemical assistance, and 17.4% under 2.0 V electrochemical assistance, which meant that permeate the fluxes were 2.2 and 3.4 times

higher than that without voltage applied, respectively. As presented in Fig. 4b, the smooth surface of these agar plates without the formation of colony suggests that bacteria were completely retained, because the pore size of *E. coli* (0.5–3 μm) was much bigger than that of MXene ultrafiltration membrane (78 nm). Improved filtration performance under electro-assistance suggests biofouling on MXene ultrafiltration membrane was mitigated by the assistance of applied negative bias potential.

NOM is ubiquitous in natural water and generally blocks membrane pores during filtration process. Therefore, natural organic matter HA was selected to examine the antifouling
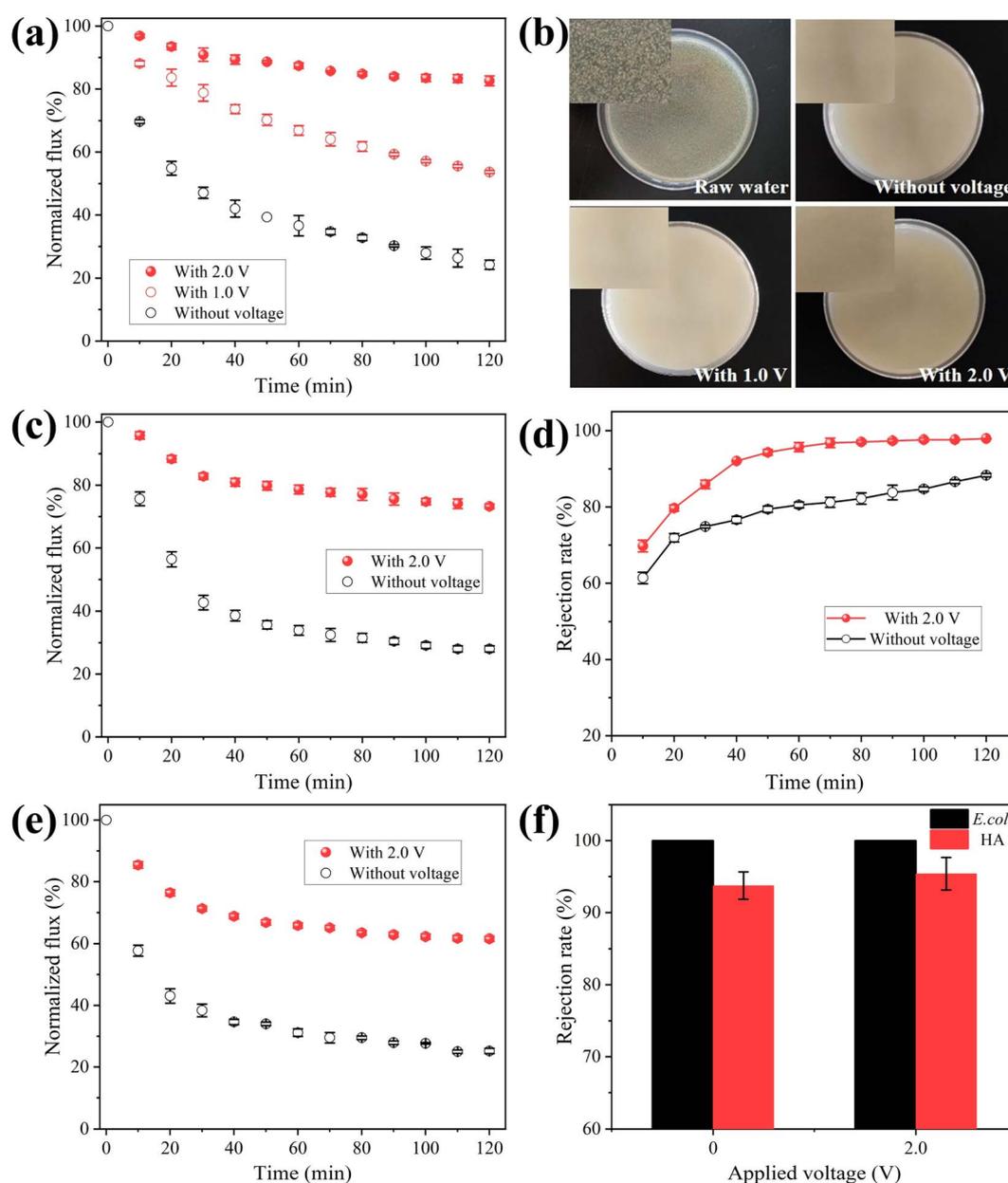
Fig. 4 (a) Normalized flux of MXene ultrafiltration membrane during filtering *E. coli* with different applied voltages, (b) coated plate photo images of raw and effluent samples during *E. coli* filtration under different applied voltages. (c) Normalized flux and (d) rejections of MXene ultrafiltration membrane during filtering NOM with running time under electro-assistance at the cell voltage of 0 and 2.0 V. (e) Normalized flux and (f) rejections of MXene ultrafiltration membrane for filtering coexisting *E. coli* and NOM at the external voltage of 0 V and 2.0 V.

performance of electrochemically assisted MXene ultrafiltration membrane. Fig. 4c presented flux decline rate of MXene ultrafiltration membrane at the cell voltage of 0 and 2.0 V. It was noted that the flux loss was 72.0% after operating for 120 min at the voltage of 0 V. However, the flux loss was decreased to 26.7% when membrane was applied with external voltage at 2.0 V, which meant that permeation flux was 2.6 times higher than that without electrochemical assistance. The decreased flux loss indicates that accumulation of HA on MXene ultrafiltration membrane was also inhibited under electrochemical assistance. Meanwhile, HA content in effluent sample was also measured. As presented in Fig. 4d, when external voltage was 0 V, HA rejection was 88.3%, however, it increased to 95.4% when external voltage was 2.0 V. The surface fouling of MXene ultrafiltration membrane was observed by SEM. As presented in Fig. S15a,† a gray HA layer was found on membrane surface when no voltage was applied, resulting in a sharp decrease in membrane flux. When applied voltage was 2.0 V, there was less NOM on membrane surface suggesting that the accumulation of NOM was mitigated (Fig. S15b†).

Since bacteria and NOM generally coexist in natural water, experiments on MXene ultrafiltration membrane were investigated using raw water containing both *E. coli* and HA. As shown in Fig. 4e, the normalized flux during 120 min running time was monitored. The flux loss was 74.8% after running for 120 min without electrochemical assistance, which indicated serious membrane fouling occurred. Under 2.0 V electrochemical assistance, the flux loss was decreased to 38.4% after 120 min filtration, which meant that permeate flux was 2.4 times higher than that without voltage applied. The increased flux indicates fouling on MXene ultrafiltration membrane was mitigated at the external voltage of 2.0 V while filtering coexisting NOM and bacteria. Meanwhile, the rejection for HA also increased to 97.3% after applying 2.0 V external voltage (Fig. 4f). From the results, the flux decreased more slowly and the rejection was higher under electrochemical assistance, resulting in an improved ability in membrane antifouling.

The result of CV measurement illustrates that no hydrogen evolution is observed on membrane at −1.0 V *vs.* Ag/AgCl and no redox peak occurs ranging from −1.2–+0.2 V *vs.* Ag/AgCl (Fig. S13†). Therefore, the electrochemical degradation of *E. coli* and HA does not occur at the cell voltage of 2.0 V. Furthermore, according to previous studies, both *E. coli* and HA molecules are negatively charged. Thus, it can be inferred that enhanced antifouling abilities and removal efficiency result from electrostatic repulsion between negatively charged contaminants and membrane under electro-assistance. As shown in Fig. 5, when the membrane was applied with negative voltage, negatively charged *E. coli* and NOM can be driven away from electronegative membrane due to the enhanced electrostatic exclusion, which led to the mitigation of membrane fouling situation and the improvement of removal efficiency. Table S1† summarizes conductive antifouling membranes reported in relevant literature. The prepared MXene membrane exhibits a high conductivity of 2×10^5 S m^{-1}. Due to its hydrophilic and negatively charged surface, MXene membrane with 2.0 V external voltage can effectively repel negatively charged humic acid (HA) molecules by enhanced electrostatic repulsion, resulting in a high rejection rate of 95%.

3.4 Performance of surface water purification

To explore the application scenario of MXene ultrafiltration membrane under electrochemical assistance, the MXene ultrafiltration membrane was utilized to purify surface water collected from a river. The indices of the water sample quality were determined and shown in Table S2.† It needed to be emphasized that the result of static adsorption experiment (Fig. S16†) showed the adsorption behavior of ceramic substrate and MXene layers made little difference toward the removal of TOC.

The change of membrane flux during filtration can reflect the degree of membrane fouling. As shown in Fig. 6a, MXene membrane flux was 232.5 L m^{-2} h^{-1} bar^{-1} after operating for 5 h with external voltage at 2.0 V, which was 1.6 times as much as that without external voltage (149.6 L m^{-2} h^{-1} bar^{-1}). The result illustrated that negative electrochemical assistance had a significant effect on alleviating membrane fouling. Notably, the removal of TOC by the MXene ultrafiltration membrane can be improved under negative electrochemical assistance (Fig. 6b). As shown in the experimental results, the removal efficiency of TOC without electrochemical assistance was 60.7%. Compared with the result of membrane without external voltage, the removal efficiency of TOC was improved to 71.2% when the membrane was served as cathode with 2.0 V voltage. The results showed negative bias had an improved effect on the separation performance of MXene ultrafiltration membrane. In order to investigate the stability of membrane coating, the membrane before and after antifouling test under electrochemical assistance was characterized by XRD. The XRD pattern did not change obviously, which indicated that the MXene membrane had good stability under electrochemical assistance (Fig. S17†). Furthermore, in terms of flux loss and effluent quality indexes (Table S3†), the integration of membrane separation and electrochemical technology is an effective strategy to improve antifouling ability and water quality.

To evaluate the regeneration ability, a negative voltage was applied to the MXene ultrafiltration membrane for cycle test. After each experiment, fouled membrane was backwashed with pure water for 30 minutes at a transmembrane pressure of 1.0 bar, while keeping the other operating conditions consistent with those of the filtration experiment. As presented in Fig. 6c, the initial flux gradually decreased throughout the cycle experiments, which indicated that different degrees of irreversible fouling occurred on membrane with or without voltage applied. After the final experiment, the membrane flux decreased by 74.2% and demonstrated unsatisfactory recovery performance. However, when external voltage was 2.0 V, membrane flux dropped slowly and maintained at more than 50% of the pure water flux, which was approximately 2.0 times higher than that without external voltage. Moreover, it needed to be emphasized that the removal rate of TOC in effluent remained stable at around 70.7% in each cycle experiment with negative electrochemical assistance (Fig. 6d). From these results, the
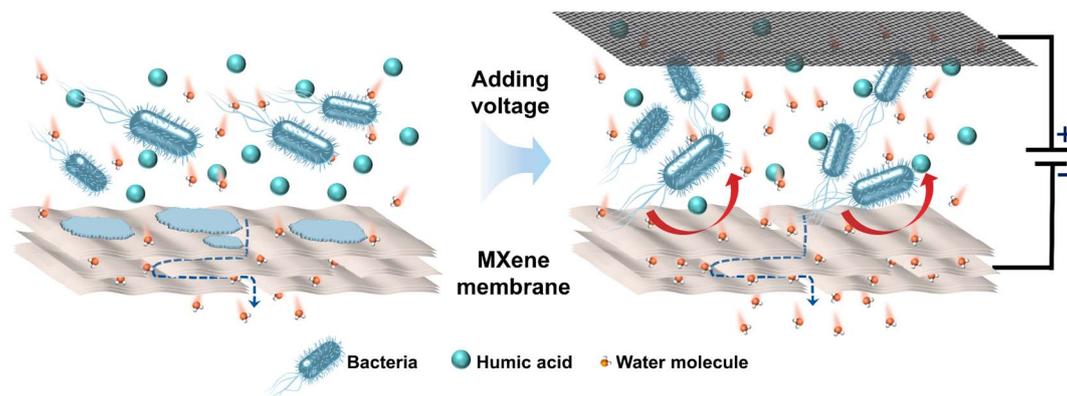
Fig. 5 Schematic diagram of membrane separation process without and with electrochemical assistance.

regeneration capability of MXene ultrafiltration membrane was improved by alleviating membrane fouling under negative electrochemical assistance.

Energy consumption in the membrane separation process is a key factor for its popularization and application. Here, specific energy consumption is calculated according to the equipment energy consumed by the total membrane water production per unit area during the operation time. The energy consumption of peristaltic pump was 3.38 kW h, and thus the specific energy consumption for membrane without external voltage was

calculated to be 0.59 kW h m^{-3}. In comparison, water production under electrochemical assistance (2.0 V, membrane as cathode) was 1.4 times higher than that without external voltage. Although the introduction of electrochemistry would increase the power consumption, the external energy consumption was only 1.71×10^{-5} kW h due to the application of 2.0 V low voltage. Thus, the specific energy consumption of membrane separation with electrochemical assistance was 0.41 kW h m^{-3}, which was 30.5% less than that without electrochemical assistance. Meanwhile, the effluent quality and water
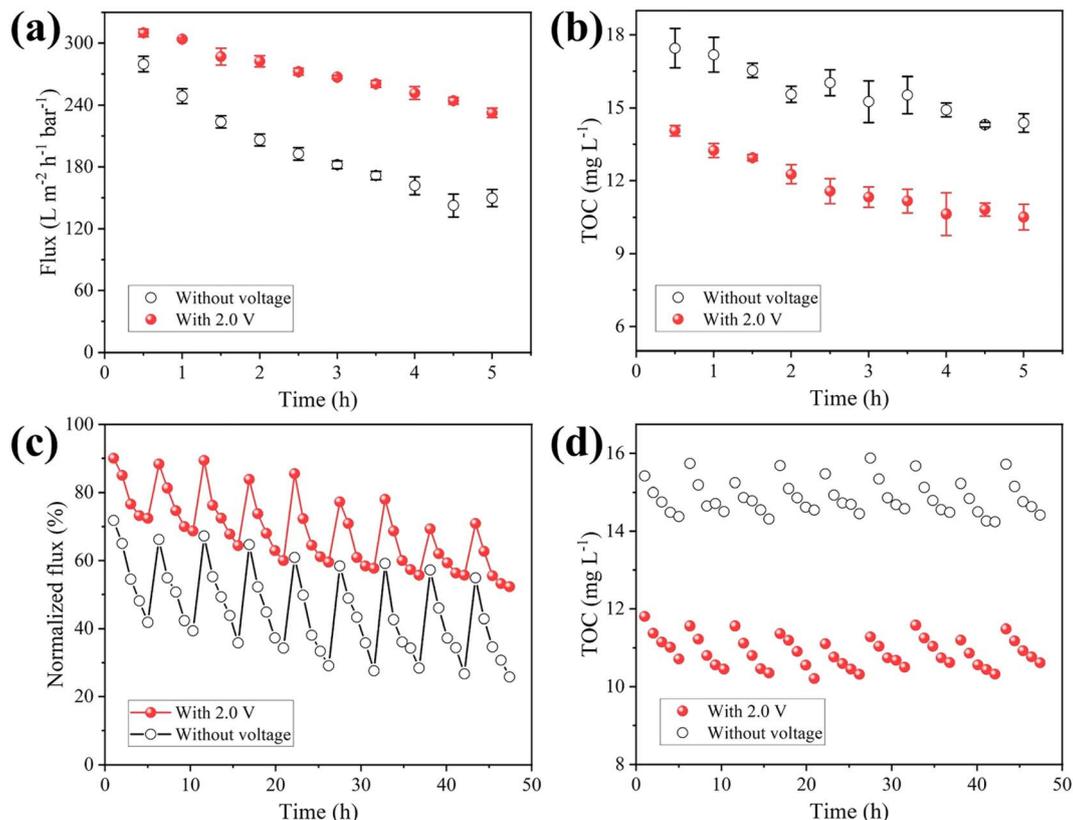

Fig. 6 (a) Membrane flux and (b) TOC content of effluent sample at the external voltage of 0 V and 2.0 V in surface water filtration, (c) flux of MXene ultrafiltration membrane and (d) TOC content of effluent sample during cycle experiment.

production has been significantly improved. Therefore, it can be considered that the electrically assisted membrane filtration process is energy-saving and high-efficiency.

4. Conclusions

In this work, an electroconductive MXene ultrafiltration membrane with good hydrophilicity has been prepared. The membrane with electrochemical assistance presented an outstanding antifouling ability for purifying water. Under negative electrochemical assistance, the permeate fluxes were 3.4 and 2.6 times as high as without electrochemical assistance in rejecting *E. coli* and HA from raw water, respectively. Furthermore, membrane fouling can also be effectively mitigated when the influent contains both *E. coli* and HA, resulting in an improved permeate flux 2.4 times higher than that without external voltage, which confirmed that negative electrochemical assistance had a positive effect on mitigating membrane fouling. Moreover, compared with results for no applied external voltage, the permeability and TOC rejection of negatively electro-assisted membrane were significantly enhanced in the treatment of surface water. It needed to be emphasized that the mitigation of membrane fouling under electrochemical assistance led to an increase in total water production, resulting in a 30.5% reduction in specific energy consumption. These results confirm that the feasibility of using negative electrochemical assistance to improve the comprehensive membrane performance, and provide basic research for its practical application.

Conflicts of interest

There are no conflicts to declare.

Acknowledgements

References

1 M. G. Buonomenna, *RSC Adv.*, 2013, **3**, 5694–5740.
2 R. N. Zhang, Y. N. Liu, M. R. He, Y. L. Su, X. T. Zhao, M. Elimelech and Z. Y. Jiang, *Chem. Soc. Rev.*, 2016, **45**, 5888–5924.
3 L. Huang, M. Zhang, C. Li and G. Q. Shi, *J. Phys. Chem. Lett.*, 2015, **6**, 2806–2815.
4 A. Lee, J. W. Elam and S. B. Darling, *Environ. Sci. Water Res. Technol.*, 2016, **2**, 17–42.
5 Q. B. Xu, Y. Liu, Y. Wang, Y. Q. Song, C. Zhao and L. Han, *Water Res.*, 2022, **210**, 117971.
6 J. Ahmad, X. H. Wen, F. J. Li and B. Wang, *RSC Adv.*, 2019, **9**, 6733–6744.
7 J. H. Jhaveri and Z. V. P. Murthy, *Desalination*, 2016, **379**, 137–154.
8 W. S. Guo, H. H. Ngo and J. X. Li, *Bioresour. Technol.*, 2012, **122**, 27–34.
9 G. L. Zhao and W. N. Chen, *RSC Adv.*, 2017, **7**, 37990–38000.
10 A. Xie, J. Cui, J. Yang, Y. Chen, J. Dai, J. Lang, C. Li and Y. Yan, *J. Mater. Chem. A*, 2019, **7**, 8491–8502.
11 B. P. Tripathi, N. C. Dubey, R. Subair, S. Choudhury and M. Stamm, *RSC Adv.*, 2016, **6**, 4448–4457.
12 S. Bano, A. Mahmood, S.-J. Kim and K.-H. Lee, *J. Mater. Chem. A*, 2015, **3**, 2065–2071.
13 Y. Yang, S. Qiao, M. Zheng, J. Zhou and X. Quan, *J. Membr. Sci.*, 2019, **582**, 335–341.
14 W. Zhang, L. Ding, J. Luo, M. Y. Jaffrin and B. Tang, *Chem. Eng. J.*, 2016, **302**, 446–458.
15 X. F. Fan, H. M. Zhao, X. Quan, Y. M. Liu and S. Chen, *Water Res.*, 2016, **88**, 285–292.
16 Y. Yang, S. Qiao, R. Jin, J. Zhou and X. Quan, *Water Res.*, 2019, **151**, 54–63.
17 L. Du, X. Quan, X. Fan, G. Wei and S. Chen, *J. Membr. Sci.*, 2020, **596**, 117613.
18 Y. Liu, G. Gao and C. D. Vecitis, *Acc. Chem. Res.*, 2020, **53**, 2892–2902.
19 X. Zhu and D. Jassby, *Acc. Chem. Res.*, 2019, **52**, 1177–1186.
20 C. M. Werner, K. P. Katuri, A. R. Hari, W. Chen, Z. Lai, B. E. Logan, G. L. Amy and P. E. Saikaly, *Environ. Sci. Technol.*, 2016, **50**, 4439–4447.
21 K. Li, M. Y. Liang, H. Wang, X. H. Wang, Y. S. Huang, J. Coelho, S. Pinilla, Y. L. Zhang, F. W. Qi, V. Nicolosi and Y. X. Xu, *Adv. Funct. Mater.*, 2020, **30**, 2000842.
22 X. D. Xu, Y. L. Zhang, H. Y. Sun, J. W. Zhou, F. Yang, H. Li, H. Chen, Y. C. Chen, Z. Liu, Z. P. Qiu, D. Wang, L. P. Ma, J. W. Wang, Q. G. Zeng and Z. Q. Peng, *Adv. Electron. Mater.*, 2021, **7**, 2000967.
23 X. L. Li, Z. D. Huang, C. E. Shuck, G. J. Liang, Y. Gogotsi and C. Y. Zhi, *Nat. Rev. Chem*, 2022, **6**, 389–404.
24 A. Shahzad, K. Rasool, W. Miran, M. Nawaz, J. Jang, K. A. Mahmoud and D. S. Lee, *ACS Sustain. Chem. Eng.*, 2017, **5**, 11481–11488.
25 P. C. Zhang, L. Wang, K. Du, S. Y. Wang, Z. W. Huang, L. Y. Yuan, Z. J. Li, H. Q. Wang, L. R. Zheng, Z. F. Chai and W. Q. Shi, *J. Hazard. Mater.*, 2020, **396**, 122731.
26 S. Kim, F. Gholamirad, M. Yu, C. M. Park, A. Jang, M. Jang, N. Taheri-Qazvini and Y. Yoon, *Chem. Eng. J.*, 2021, **406**, 126789.
27 P. Y. Kuang, J. X. Low, B. Cheng, J. G. Yu and J. J. Fan, *J. Mater. Sci. Technol.*, 2020, **56**, 18–44.
28 S. Iravani and R. S. Varma, *Molecules*, 2022, **27**, 6939.
29 O. Kwon, Y. Choi, J. H. Kang, J. H. Kim, E. Choi, Y. C. Woo and D. W. Kim, *Desalination*, 2022, **522**, 115448.
30 L. Ding, Y. Y. Wei, Y. J. Wang, H. B. Chen, J. Caro and H. H. Wang, *Angew. Chem., Int. Ed.*, 2017, **56**, 1825–1829.
31 H. E. Karahan, K. Goh, C. F. Zhang, E. Yang, C. Yildirim, C. Y. Chuah, M. G. Ahunbay, J. Lee, S. B. Tantekin-Ersolmaz, Y. Chen and T. H. Bae, *Adv. Mater.*, 2020, **32**, 1906697.
32 X. F. Fan, H. M. Zhao, Y. M. Liu, X. Quan, H. T. Yu and S. Chen, *Environ. Sci. Technol.*, 2015, **49**, 2293–2300.
33 X. B. Zhu and D. Jassby, *Acc. Chem. Res.*, 2019, **52**, 1177–1186.
34 L. Ding, L. B. Li, Y. C. Liu, Y. Wu, Z. Lu, J. J. Deng, Y. Y. Wei, J. Caro and H. H. Wang, *Nat. Sustain.*, 2020, **3**, 296–302.

35 T. Liu, X. Y. Liu, N. Graham, W. Z. Yu and K. N. Sun, *J. Membr. Sci.*, 2020, **593**, 1906697.

36 S. J. Gao, Y. Z. Zhu, Y. Q. Gong, Z. Y. Wang, W. X. Fang and J. Jin, *ACS Nano*, 2019, **13**, 5278–5290.

37 X. F. Shi, G. Tal, N. P. Hankins and V. Gitis, *J. Water Process Eng.*, 2014, **1**, 121–138.

38 N. Li, T. J. Lou, W. Y. Wang, M. Li, Z. X. Yang, R. Y. Chang, J. X. Li and H. Z. Geng, *J. Membr. Sci.*, 2023, **668**, 121271.

39 M. Alhabeb, K. Maleski, B. Anasori, P. Lelyukh, L. Clark, S. Sin and Y. Gogotsi, *Chem. Mater.*, 2017, **29**, 7633–7644.

40 M. Naguib, M. Kurtoglu, V. Presser, J. Lu, J. J. Niu, M. Heon, L. Hultman, Y. Gogotsi and M. W. Barsoum, *Adv. Mater.*, 2011, **23**, 4248–4253.

41 J. Halim, K. M. Cook, M. Naguib, P. Eklund, Y. Gogotsi, J. Rosen and M. W. Barsoum, *Appl. Surf. Sci.*, 2016, **362**, 406–417.

42 O. Mashtalir, M. Naguib, V. N. Mochalin, Y. Dall'Agnese, M. Heon, M. W. Barsoum and Y. Gogotsi, *Nat. Commun.*, 2013, **4**, 1716.

43 M. Ghidiu, M. R. Lukatskaya, M. Q. Zhao, Y. Gogotsi and M. W. Barsoum, *Nature*, 2014, **516**, 78–81.

44 G. Z. Liu, J. Shen, Q. Liu, G. P. Liu, J. Xiong, J. Yang and W. Q. Jin, *J. Membr. Sci.*, 2018, **548**, 548–558.